

Drying Pathways of an Evaporating Soft Matter Droplet

Guangle Du,^{1,2,3} Fangfu Ye,^{2,3,4,5} Masao Doi,⁶ and Fanlong Meng^{1,*}

¹CAS Key Laboratory of Theoretical Physics, Institute of Theoretical Physics, Chinese Academy of Sciences, Beijing 100190, China

²Wenzhou Institute, University of Chinese Academy of Sciences, Wenzhou, Zhejiang 325001, China

³School of Physical Sciences, University of Chinese Academy of Sciences, Beijing 100049, China

⁴Beijing National Laboratory for Condensed Matter Physics,

Institute of Physics, Chinese Academy of Sciences, Beijing 100190, China

⁵Songshan Lake Materials Laboratory, Dongguan, Guangdong 523808, China

⁶Center of Soft Matter Physics and its Applications, Beihang University, Beijing 100191, China

(Dated: June 19, 2020)

Micro-droplets of soft matter solutions have different morphologies upon drying, and can finally become wrinkled, buckled or cavitated particles. We investigate the morphology evolution of a drying soft matter droplet in this work: at the early stage of drying, wrinkling or cavitation instability can occur in the droplet, depending on the comparison between the critical wrinkling and cavitation pressure; at a later stage of drying, no wrinkle will appear if cavitation happens first, while there can still be cavitation if wrinkling happens first. A three-dimensional phase diagram in the space of elastic length, gel layer thickness and weight loss is provided for illustrating these drying pathways of a soft matter droplet, which can guide future fabrications of micro-particles with desired morphologies.

A soft matter droplet consisting of polymer solutions or colloidal dispersions can exhibit different morphologies such as buckling [1–4], wrinkling [5–8], or cavitation [9–12] during the drying process. When all solvents evaporate, the soft matter droplets can turn out to be solid, hollow, wrinkled or buckled particles as the final products [13–17]. This drying process, especially spray drying, has been widely utilised to produce micro-particles of different morphologies in industrial circumstances such as food or pharmaceutical particle production [17–21], amorphous material crystallisation [22–24], functional encapsulated particle manufacture [25–27], *etc.*, where different shapes are achieved by empirically changing the drying temperature, concentration and constitution of the soft matter solution [3, 28–34].

In the drying process of a soft matter droplet, the competition of solute deposition on the droplet surface due to drying and solute diffusion homogenising the solute concentration is captured by the dimensionless evaporating Péclet number. When Péclet number is sufficiently large, the solution at the outmost layer of the droplet can solidify to be a gel-like layer [16, 35–37], which can grow with time. This gel layer has been believed as related with the morphology evolution and the final configurations of drying soft matter droplets [12, 31, 38–40]. However, how the properties of the gel layer can determine the drying process of the soft matter droplet still remains unclear.

In this work, we will study how the morphology of a drying soft matter droplet can evolve with time depending on the physical properties of the gel layer such as its elasticity and dimension, by considering the prepared state of the droplet as a spherical core-shell structured system as in spray drying [shown in Fig. 1(a)]. The core will be simply regarded as liquid, whose amount decreases continuously due to evaporation; the shell (skin

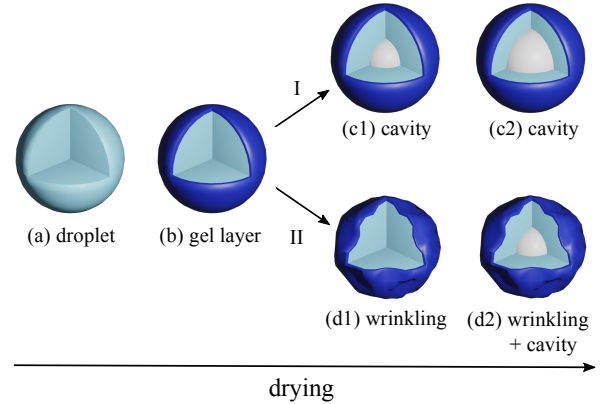


FIG. 1. Drying pathways of an evaporating soft matter droplet.

layer) will be treated with non-evolving elastic properties and thickness here for simplicity, as the evolution of the skin layer, such as mass growing from further diffusion and deposition of the solute, would not change the results qualitatively. By taking these simplifications, we can construct the analytical energy form of the system, and then discuss the morphology evolution of the drying soft matter droplet.

Compared to solvent evaporation, the mechanically equilibrating process of the gel layer is a fast process; in other words, we can use the mass loss of the droplet due to evaporation, $\Delta W = W_0 - W$, as the controllable variable of the system, where W_0 and W denote the initial and current mass of the droplet, respectively. Then we can discuss the morphology evolution of the droplet by optimising the total free energy of the system under given ΔW . By taking the initial radius of the droplet as

R_0 , and the radius of the cavity as R_c [reduced cavity volume $v_c \equiv (R_c/R_0)^3$], the volume of droplet can be expressed as $V = 4\pi R_0^3(1 - \Delta W/W_0 + v_c)/3$ from volume conservation. The total Gibbs free energy of the system can be written as

$$F_{\text{tot}}(u_\alpha, w, v_c; \Delta W) = 4\pi R_0^2 \gamma v_c^{2/3} + \frac{4\pi R_0^3}{3} \Delta p_{lc} v_c \quad (1)$$

$$+ \int dS \left[\frac{1}{2} (E_{\alpha\beta} N^{\alpha\beta} + K_{\alpha\beta} M^{\alpha\beta}) - \Delta p_{ol} w \right],$$

where $\Delta p_{ol} = p_o - p_l$ and $\Delta p_{lc} = p_l - p_c$, with $p_o \sim 10^5$ Pa, p_l and p_c as the pressure of the outside, the liquid and the cavity, respectively. The pressure of the cavity can be expressed as $p_c = -k_B T / v_l \cdot W_0 \left(-\frac{p_{\text{eq}} v_l}{k_B T} e^{-\frac{p_{\text{eq}} v_l}{k_B T} - \frac{2\gamma v_l}{R_c k_B T}} \right)$ [41], where v_l is the volume of a single liquid molecule, $W_0(x)$ is Lambert W function and p_{eq} is the vapor pressure in the bulk. Taking typical values of $v_l \sim 10^{-29}$ m³ and $p_{\text{eq}} \sim 10^5$ Pa, we have $p_{\text{eq}} v_l / (k_B T) \sim 10^{-3}$, and then the pressure of cavity can be approximated by $p_c \approx p_{\text{eq}} \exp[-2\gamma v_l / (R_c k_B T)]$. In Equation (1), the first term on the right-hand-side (RHS) denotes the interfacial energy of the interface between cavity and liquid, the second term denotes the work done by the pressure difference between the liquid and the cavity, and the last term denotes the elastic energy of the gel layer. In the last term, $E^{\alpha\beta}$ and $K^{\alpha\beta}$ are the stretching and the bending strains, respectively, $N^{\alpha\beta}$ and $M^{\alpha\beta}$ are the stretching stress and the bending moment, respectively, w is the normal displacement along the radial direction of the gel layer. Note that we have taken inward normal displacement as positive. Here we adopt the Donnell-Mushtari-Vlasov (DMV) strain-displacement relations, which are valid for small deformations, as $E_{\alpha\beta} = (\nabla_\beta u_\alpha + \nabla_\alpha u_\beta)/2 - b_{\alpha\beta} w + \partial_\alpha w \partial_\beta w/2$ and $K_{\alpha\beta} = \nabla_\alpha \nabla_\beta w$, where ∇ is covariant derivative, u_α is the tangential displacement along α direction and $b_{\alpha\beta}$ is curvature tensor of the gel layer shell [42]. The stretching stress $N^{\alpha\beta}$ and the bending moment $M^{\alpha\beta}$ can be expressed as functions of the strain tensors: $N^{\alpha\beta} = Eh[(1 - \nu)E^{\alpha\beta} + \nu g^{\alpha\beta} E^\gamma_\gamma] / (1 - \nu^2)$ and $M^{\alpha\beta} = Eh^3[(1 - \nu)K^{\alpha\beta} + \nu g^{\alpha\beta} K^\gamma_\gamma] / [12(1 - \nu^2)]$, with $g^{\alpha\beta}$ being the metric tensor of shell surface, and h , E and ν being the thickness, Young's modulus and the Poisson's ratio of the gel layer, respectively [42].

Critical wrinkling pressure. The gel layer can wrinkle or buckle during the drying process, and we first discuss the criterion of when wrinkling or buckling can occur in the droplet. If there is no cavity, the total energy reduces to the purely elastic one [last term on RHS of Equation (1)]. To obtain the critical wrinkling pressure, we can perform the linear instability analysis on the Euler-Lagrange (EL) equations obtained from the optimisation of the elastic energy [41]. First, the uniform solution of EL equations is $u_\phi = u_\theta = 0$, $w_0 = (1 - \nu)\Delta p_{ol} R_0^2 / (2Eh)$, which represents the uniform contraction of the gel layer

under the pressure difference between outside and liquid Δp_{ol} . By adding a small perturbation w_1 in the normal displacement with the total modified normal displacement as $w = w_0 + w_1$ and introducing a small perturbation χ_1 in the Airy stress function [42], we can obtain

$$\frac{Eh^3}{12(1 - \nu^2)} \Delta^2 w_1 - \frac{1}{R_0} \Delta \chi_1 + \frac{\Delta p_{ol} R_0}{2} \Delta w_1 = 0, \quad (2a)$$

$$\frac{1}{Eh} \Delta^2 \chi_1 + \frac{1}{R_0} \Delta w_1 = 0, \quad (2b)$$

after keeping terms up to the linear order in the EL equations. By expressing w_1 and χ_1 with spherical harmonics $Y_l^m(\phi, \theta)$ (eigenmodes of Laplace operator), as $w_1 = AY_l^m$ and $\chi_1 = BY_l^m$, then from Equation (2) we can obtain the possible eigenmodes denoted by l as a function of the pressure Δp_{ol} ,

$$l(l+1) = \frac{\Delta p_{ol} R_0^3}{4D} \left(1 \pm \sqrt{1 - \frac{16DEh}{(\Delta p_{ol})^2 R_0^4}} \right), \quad (3)$$

where $D = Eh^3/[12(1 - \nu^2)]$. The minimal pressure p_w^* to have a real and positive $l(l+1)$, *i.e.*, the critical pressure leading to wrinkling, is [42]

$$p_w^* = \frac{2E}{\sqrt{3(1 - \nu^2)}} \left(\frac{h}{R_0} \right)^2, \quad (4)$$

illustrating that the gel layer can easily wrinkle if the gel layer is soft (small Young's modulus) and thickness is small compared to the droplet size. If there is a ring-like defect with a smaller Young's modulus in the gel layer, then buckling can easily happen and the corresponding buckling pressure can be obtained by shallow shell approximation, which gives the same value as the critical wrinkling pressure p_w^* [41]. Note this critical wrinkling pressure is obtained for perfect sphere and is sensitive to imperfections [43, 44]. If imperfections are present in shell possibly due to density inhomogeneity [45], orthotropic elasticity [46], *etc.*, the critical wrinkling pressure can drop a lot by an empirical proportion. Nevertheless, the above critical wrinkling pressure can still dominate the wrinkling behavior. In the following discussions, we will keep the term 'wrinkling instability' for denoting both wrinkling and buckling instability without losing generality.

Critical cavitation pressure. Meanwhile, there is a critical cavitation pressure p_c^* supposing that there is no wrinkling. In this case, the elastic energy of the gel layer is simply $F_{\text{elastic}} = 12\pi h K_e w_0^2$ [39], where $K_e = E/[3(1 - \nu)]$ is an effective elastic modulus. After the insertion of the mass conservation relation, the

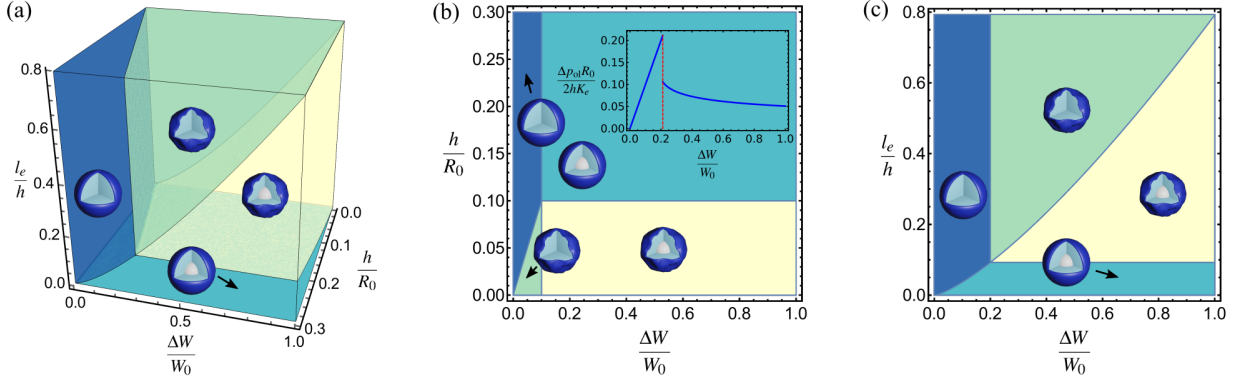


FIG. 2. (a) 3D phase diagram with three dimensionless varying variables, *i.e.*, elastic length over shell thickness l_e/h , shell thickness over initial droplet radius h/R_0 , and the reduced weight loss of the droplet $\Delta W/W_0$. Here Poisson ratio $\nu = 0.5$. (b) Cross section of 3D phase diagram with fixed $l_e/h = 0.037$ demonstrating one of the two drying pathways. Namely when the shell is thick enough, cavity develops with increase of weight loss. Inset: the pressure difference between outside and liquid is smaller than the critical cavitation pressure and constantly decreases after cavitation, impeding the occurrence of wrinkling. In the inset, $l_e/h = 0.1$. (c) Cross section of 3D phase diagram with fixed $h/R_0 = 0.2$ showing the other drying pathway, *i.e.*, from gel layer to wrinkling to both wrinkling and cavitation with high elastic length l_e .

total Gibbs free energy of the system is

$$F_{\text{tot}}(v_c; \Delta W) = 4\pi R_0^2 \gamma v_c^{2/3} + \frac{4\pi R_0^3}{3} \Delta p_{\text{oc}} v_c \quad (5) \\ + \frac{4\pi R_0^2 h K_e}{3} \left(v_c - \frac{\Delta W}{W_0} \right)^2,$$

where $\Delta p_{\text{oc}} = p_o - p_c$. The critical point for the above total Gibbs free energy to have a non-zero local minimum point is determined by $\partial F_{\text{tot}}/\partial v_c = 0$ and $F_{\text{tot}}(v_c) = F_{\text{tot}}(0)$, from which we can obtain the critical cavity volume as $v_c^* = [l_e/(2h)]^{3/4}$ with the elastic length defined by $l_e \equiv 2\gamma/K_e$ and critical weight loss for cavitation as $\Delta W^*/W_0 = [2 + p_{\text{eq}}v_l/(k_B T)]v_c^*$ [39]. Utilisation of the mass conservation under uniform contraction with no cavity gives us the relation between pressure and weight loss $\Delta p_{\text{ol}} = 2hK_e/R_0 \cdot \Delta W/W_0$. Then the critical cavitation pressure is

$$p_c^* = \frac{4hK_e}{R_0} \left(1 + \frac{p_{\text{eq}}v_l}{2k_B T} \right) \left(\frac{l_e}{2h} \right)^{3/4}. \quad (6)$$

By comparing the critical wrinkling pressure p_w^* and the critical cavitation pressure p_c^* , we can obtain the criterion for wrinkling happening ahead of the droplet cavitation at the early stage of the drying process, as

$$\left(\frac{2}{9} \right)^{1/4} \left(\frac{1+\nu}{1-\nu} \right)^{1/2} \left(1 + \frac{p_{\text{eq}}v_l}{2k_B T} \right) \frac{R_0}{h} \left(\frac{l_e}{h} \right)^{3/4} > 1; \quad (7)$$

otherwise, cavitation occurs first. In other words, if the gel layer is thin and soft, the droplet tends to wrinkle at the surface. More importantly, such divergence in the onset instabilities at the early stage of the drying process leads to different drying pathways and can determine the final morphology of the drying droplet as discussed below.

Drying pathway—no wrinkling after cavitation. First we investigate whether wrinkling still occurs if cavitation happens first. This can be answered by understanding how the pressure difference between outside and liquid Δp_{ol} changes with the increase of weight loss ΔW . As shown in the inset of Fig. 2 (b), Δp_{ol} constantly increases before cavitation and becomes $2\gamma[1 + p_{\text{eq}}v_l/(k_B T)]v_c^{-1/3}/R_0$ after cavitation. At the critical cavitation point, $\Delta p_{\text{ol}} = 2hK_e/R_0 \cdot [1 + p_{\text{eq}}v_l/(k_B T)][l_e/(2h)]^{3/4}$, which is smaller than the critical cavitation pressure p_c^* . Meanwhile, the first derivative of Δp_{ol} after cavitation with regards to the weight loss, $\partial \Delta p_{\text{ol}}/\partial \Delta W = -2\gamma/(R_0 W_0) \cdot 1/[3[1 + p_{\text{eq}}v_l/(k_B T)]^{-1}v_c^{4/3} - v_c^{*4/3}] < 0$, means that Δp_{ol} decreases further with increasing weight loss ΔW , indicating no wrinkling can happen after cavitation since the critical wrinkling pressure can not be reached any more [drying pathway in Fig. 1 as (a) \rightarrow (b) \rightarrow (c1) \rightarrow (c2)].

Drying pathway—cavitation after wrinkling. We proceed to investigate whether the cavity can still form if wrinkling occurs first. By assuming wrinkling as a perturbation of a single spherical harmonic mode and the perturbation amplitude is small, then the Helmholtz free energy can be expressed in the same form as that in equation (5), but with a modified effective elastic modulus [41]

$$K_e' = K_e \left[1 - \frac{3(1+\nu)A^2}{8\pi} \right], \quad (8)$$

where $A' = A/h$ is the ratio of the perturbation amplitude over the gel layer thickness. Then the problem of whether cavitation can happen after wrinkling, is reduced to if cavitation can happen under uniform contraction with the new elastic modulus K_e' . Then we can obtain the new critical weight loss for cavitation, namely, $\Delta W'/W_0 = [l_e'/(2h)]^{3/4}$, where $l_e' \equiv 2\gamma/K_e'$ is the new

elastic length. Thus cavitation can still happen after wrinkling, when the weight loss exceeds the above critical value. Meanwhile, the effective elastic modulus K'_e is smaller than the one without wrinkling K_e , resulting in a larger value of the critical weight loss than that in the case without wrinkling. Note that according to the previous discussion, the pressure difference between outside and liquid Δp_{ol} drops at cavitation and constantly decreases after cavitation with the increase of weight loss [see inset of Fig. 2(b)], thus the wrinkles may disappear due to the decrease of Δp_{ol} . However, in practical drying process, the formed wrinkles of the gel layer can become rigid, *e.g.* turning glassy [38], and the decrease of Δp_{ol} induced by the cavitation is not high enough to flatten the wrinkles on the gel layer with increased rigidity. In this case, the wrinkles can still remain regardless of the decrease of pressure difference between outside and liquid after cavitation [drying pathway in Fig. 1 as (a) \rightarrow (b) \rightarrow (d1) \rightarrow (d2)]. Note that the gel layer can still be permeable to solvent despite of rigidification. Thus the subsequent evaporation and cavity enlargement are not hindered.

In Fig. 2(a), a 3D phase diagram summarising the above discussions of the drying pathways of a soft matter droplet is provided in the space of (elastic length, gel layer thickness and weight loss), together with its two cross sections of given fixed elastic length in Fig. 2(b) and of given fixed thickness in Fig. 2(c), respectively. Note that the weight loss in the phase diagram can play the role of time if the evaporation rate of the droplet is known [37, 47]. At the early stage of the drying process, *i.e.*, when ΔW is small, either wrinkling or cavitation instability can occur, resulting from the competition between the surface energy of the cavity, and the bending and the stretching elastic energy of the gel layer. When the gel layer is thin and soft [small h and small K_e (large l_e)], then wrinkling occurs, which is obvious in Fig. 2(b) and Fig. 2(c); otherwise, cavitation happens. Meanwhile, the choice in either wrinkling or cavitation instability at the early stage of the drying process, determines the later morphology evolution and the final product of the drying soft matter droplet: (a) if wrinkling takes place ahead of the cavitation, then there will still be cavity formed in the droplet with the ongoing evaporation of the solvents and the final configuration of the drying droplet will be a hollow and wrinkled particle; (b) if cavitation happens first, then there will be no wrinkling in the later drying process due to the decreasing pressure difference between the outside and the droplet, and a spherical shell is left after finishing the whole evaporation process.

We here investigate how the morphology of a drying soft matter droplet can evolve with time based on a pseudo-dynamic analysis. The elastic properties of the gel layer formed at the surface of the soft matter droplet play the key role in determining the drying pathways of the droplet, including both the instabilities triggered at

the early stage of the drying process, the later morphology evolution, and the final configurations. Although simplifications like the non-evolving gel layer have been made for analytic discussions, we believe this portable model has captured the essential physics underlying the morphology evolution of a drying soft matter droplet, which can guide the industrial fabrications of micro-particles with desired morphologies and functions.

F.Y. acknowledges the support of the National Natural Science Foundation of China (Grant No. 11774394) and the Key Research Program of Frontier Sciences of Chinese Academy of Sciences (Grant No. QYZDB-SSW-SYS003). G.D. thanks Xiao Lin for fruitful discussions.

* fanlong.meng@itp.ac.cn

- [1] N. Tsapis, E. Dufresne, S. Sinha, C. Riera, J. Hutchinson, L. Mahadevan, and D. Weitz, *Phys. Rev. Lett.* **94**, 018302 (2005).
- [2] F. Boulogne, F. Giorgiutti-Dauphiné, and L. Pauchard, *Soft Matter* **9**, 750 (2013).
- [3] B. Pathak and S. Basu, *J. Appl. Phys.* **117**, 244901 (2015).
- [4] M. S. Tirumkudulu, *Soft Matter* **14**, 7455 (2018).
- [5] E. Rio, A. Daerr, F. Lequeux, and L. Limat, *Langmuir* **22**, 3186 (2006).
- [6] Y. Zhang, Y. Qian, Z. Liu, Z. Li, and D. Zang, *Eur. Phys. J. E* **37**, 84 (2014).
- [7] H. M. van der Kooij, G. T. van de Kerkhof, and J. Sprakel, *Soft Matter* **12**, 2858 (2016).
- [8] S. Zheng, S. Huang, L. Xiong, W. Yang, Z. Liu, B. Xie, and M. Yang, *Eur. Polym. J.* **104**, 99 (2018).
- [9] S. Arai and M. Doi, *Eur. Phys. J. E* **35**, 57 (2012).
- [10] C. Sadek, H. Tabuteau, P. Schuck, Y. Fallourd, N. Pradeau, C. Le Floch-Fouéré, and R. Jeantet, *Langmuir* **29**, 15606 (2013).
- [11] L. Bansal, A. Miglani, and S. Basu, *Phys. Rev. E* **93**, 042605 (2016).
- [12] L. Bansal, P. Seth, S. Sahoo, R. Mukherjee, and S. Basu, *Appl. Phys. Lett.* **113**, 213701 (2018).
- [13] D. Walton and C. Mumford, *Chem. Eng. Res. Des.* **77**, 442 (1999).
- [14] D. Walton, *Drying Technol.* **18**, 1943 (2000).
- [15] J. Elversson, A. Millqvist-Fureby, G. Alderborn, and U. Elofsson, *J. Pharm. Sci.* **92**, 900 (2003).
- [16] R. Vehring, W. R. Foss, and D. Lechuga-Ballesteros, *J. Aerosol Sci.* **38**, 728 (2007).
- [17] R. Vehring, *Pharm. Res.* **25**, 999 (2008).
- [18] S. H. Anwar and B. Kunz, *J. Food Eng.* **105**, 367 (2011).
- [19] S. Giovagnoli, F. Palazzo, A. D. Michele, A. Schoubben, P. Blasi, and M. Ricci, *J. Pharm. Sci.* **103**, 1255 (2014).
- [20] M. R. I. Shishir and W. Chen, *Trends Food Sci. Technol.* **65**, 49 (2017).
- [21] S. Huang, M.-L. Vignolles, X. D. Chen, Y. Le Loir, G. Jan, P. Schuck, and R. Jeantet, *Trends Food Sci. Technol.* **63**, 1 (2017).
- [22] R. Price and P. M. Young, *J. Pharm. Sci.* **93**, 155 (2004).
- [23] D. Chiou and T. Langrish, *Drying Technol.* **25**, 1427 (2007).
- [24] D. Chiou and T. Langrish, *J. Food Eng.* **88**, 177 (2008).

- [25] M. I Ré, *Drying Technol.* **16**, 1195 (1998).
- [26] B. N. Estevinho, F. Rocha, L. Santos, and A. Alves, *Trends Food Sci. Technol.* **31**, 138 (2013).
- [27] A. Trojanowska, A. Nogalska, R. G. Valls, M. Giamberini, and B. Tylkowski, *Phys. Sci. Rev.* **2**, 20170020 (2017).
- [28] F. Iskandar, L. Gradon, and K. Okuyama, *J. Colloid Interface Sci.* **265**, 296 (2003).
- [29] D. Sen, J. S. Melo, J. Bahadur, S. Mazumder, S. Bhat-tacharya, S. F. D'Souza, H. Frielinghaus, G. Goerigk, and R. Loidl, *Soft Matter* **7**, 5423 (2011).
- [30] É. Lintingre, G. Ducouret, F. Lequeux, L. Olanier, T. Périé, and L. Talini, *Soft Matter* **11**, 3660 (2015).
- [31] E. Lintingre, F. Lequeux, L. Talini, and N. Tsapis, *Soft Matter* **12**, 7435 (2016).
- [32] B. Pathak and S. Basu, *Langmuir* **32**, 2591 (2016).
- [33] P. Biswas, D. Sen, S. Mazumder, C. Basak, and P. Doshi, *Langmuir* **32**, 2464 (2016).
- [34] L. T. Raju, S. Chakraborty, B. Pathak, and S. Basu, *Langmuir* **34**, 5323 (2018).
- [35] T. Okuzono, K. Ozawa, and M. Doi, *Physical Review Letters* **97**, 136103 (2006).
- [36] K. L. Maki and S. Kumar, *Langmuir* **27**, 11347 (2011).
- [37] F. Meng, L. Luo, M. Doi, and Z. Ouyang, *Eur. Phys. J. E* **39**, 22 (2016).
- [38] L. Pauchard and C. Allain, *Europhys. Lett.* **62**, 897 (2003).
- [39] F. Meng, M. Doi, and Z. Ouyang, *Phys. Rev. Lett.* **113**, 098301 (2014).
- [40] C. Sadek, P. Schuck, Y. Fallourd, N. Pradeau, R. Jean-tet, and C. Le Floch-Fouéré, *Food Hydrocolloids* **52**, 161 (2016).
- [41] See supplementary materials.
- [42] F. Niordson, *Shell Theory* (Nord-Holland, Amsterdam, 1985).
- [43] J. M. T. Thompson, *Int. J. Bifurcation Chaos* **25**, 1530001 (2015).
- [44] J. W. Hutchinson, *Proc. R. Soc. A* **472**, 20160577 (2016).
- [45] S. S. Datta, S.-H. Kim, J. Paulose, A. Abbaspourrad, D. R. Nelson, and D. A. Weitz, *Phys. Rev. Lett.* **109**, 134302 (2012).
- [46] G. Munglani, F. K. Wittel, R. Vetter, F. Bianchi, and H. J. Herrmann, *Phys. Rev. Lett.* **123**, 058002 (2019).
- [47] M. A. Boraey and R. Vehring, *J. Aerosol Sci.* **67**, 131 (2014).

Drying Pathways of an Evaporating Soft Matter Droplet

Supplemental Material

Guangle Du,^{1,2,3} Fangfu Ye,^{2,3,4,5} Masao Doi,⁶ and Fanlong Meng^{1,*}

¹*CAS Key Laboratory of Theoretical Physics, Institute of Theoretical Physics,
Chinese Academy of Sciences, Beijing 100190, China*

²*Wenzhou Institute, University of Chinese Academy
of Sciences, Wenzhou, Zhejiang 325001, China*

³*School of Physical Sciences, University of Chinese
Academy of Sciences, Beijing 100049, China*

⁴*Beijing National Laboratory for Condensed Matter Physics,
Institute of Physics, Chinese Academy of Sciences, Beijing 100190, China*

⁵*Songshan Lake Materials Laboratory,
Dongguan, Guangdong 523808, China*

⁶*Center of Soft Matter Physics and its Applications,
Beihang University, Beijing 100191, China*

* fanlong.meng@itp.ac.cn

I. DERIVATION OF EULER-LAGRANGE EQUATIONS

In this section, we give the detailed derivation of Euler-Lagrange equations from the elastic free energy of shell

$$F_{\text{elastic}}(u_\alpha, w) = \int_S dS \left[\frac{1}{2} (E_{\alpha\beta} N^{\alpha\beta} + K_{\alpha\beta} M^{\alpha\beta}) - \Delta p_{\text{ol}} w \right], \quad (\text{S1})$$

where Δp_{ol} is pressure difference between outside and liquid, *i.e.*, net pressure exerted on the shell. u_α and w are, respectively, tangential and normal displacements on the gel layer shell. $E_{\alpha\beta}$ and $K_{\alpha\beta}$ are, respectively, the stretching and bending strains. $N^{\alpha\beta}$ and $M^{\alpha\beta}$ are stretching stress and bending moment, which can be written in terms of stretching and bending strains [1]

$$N^{\alpha\beta} = \frac{Eh}{1-\nu^2} [(1-\nu)E^{\alpha\beta} + \nu g^{\alpha\beta} E_\gamma^\gamma], \quad (\text{S2})$$

$$M^{\alpha\beta} = \frac{Eh^3}{12(1-\nu^2)} [(1-\nu)K^{\alpha\beta} + \nu g^{\alpha\beta} K_\gamma^\gamma], \quad (\text{S3})$$

with $g^{\alpha\beta}$ being metric tensor of shell surface and h , E and ν being thickness, Young's modulus and Poisson's ratio of shell. We adopt here the DonnellMushtariVlasov (DMV) strain-displacement relations [1]

$$E_{\alpha\beta} = \frac{1}{2} (\nabla_\beta u_\alpha + \nabla_\alpha u_\beta) - b_{\alpha\beta} w + \frac{1}{2} \partial_\alpha w \partial_\beta w, \quad (\text{S4})$$

$$K_{\alpha\beta} = \nabla_\alpha \nabla_\beta w, \quad (\text{S5})$$

where $b_{\alpha\beta}$ is curvature tensor and ∇ is covariant derivative. Note in the elastic free energy Eq. (S1), there is second order derivative of w . In general curved space, the Euler-Lagrange equations are

$$\frac{\partial f_{\text{elastic}}}{\partial u_\alpha} - \nabla_\beta \frac{\partial f_{\text{elastic}}}{\partial \nabla_\beta u_\alpha} = 0, \quad (\text{S6})$$

$$\frac{\partial f_{\text{elastic}}}{\partial w} - \nabla_\alpha \frac{\partial f_{\text{elastic}}}{\partial \partial_\alpha w} + \nabla_\beta \nabla_\alpha \frac{\partial f_{\text{elastic}}}{\partial \partial_\alpha \partial_\beta w} = 0, \quad (\text{S7})$$

where f_{elastic} is the elastic free energy density. Then

$$\nabla_\beta N^{\alpha\beta} = 0, \quad (\text{S8})$$

$$-N^{\alpha\beta} b_{\alpha\beta} - \Delta p_{\text{ol}} - N^{\alpha\beta} \nabla_\alpha \nabla_\beta w + \nabla_\beta \nabla_\alpha M^{\alpha\beta} = 0. \quad (\text{S9})$$

An auxiliary function called Airy stress function can be introduced to reduce the above three equations into two equations. Let $N^{\alpha\beta} \equiv \varepsilon^{\alpha\gamma} \varepsilon^{\beta\delta} \nabla_\gamma \nabla_\delta \chi$. According to the formula

$$\nabla_\alpha \nabla_\beta A^\gamma - \nabla_\beta \nabla_\alpha A^\gamma = A^\delta R^\gamma_{\delta\alpha\beta}, \quad (\text{S10})$$

where $R^\alpha_{\beta\gamma\delta}$ is Riemann curvature tensor and on 2D surface

$$R^\alpha_{\beta\gamma\delta} = K(g_\gamma^\alpha g_{\beta\delta} - g_\delta^\alpha g_{\beta\gamma}), \quad (\text{S11})$$

where K is Gauss curvature,

$$\nabla_\alpha \nabla_\beta A^\gamma = \frac{1}{2}(\nabla_\alpha \nabla_\beta + \nabla_\beta \nabla_\alpha)A^\gamma + \frac{1}{2}K(A_\beta g_\alpha^\gamma - A_\alpha g_\beta^\gamma). \quad (\text{S12})$$

Denote the characteristic length of deformation with l . The first symmetric part on the right hand side is of order $1/l^2$ and the second anti-symmetric part is of order K . If we assume $1/l^2 \gg K$, *i.e.*, the inverse of characteristic length of deformation squared is far larger than Gauss curvature, then the second anti-symmetric part can be omitted and only the first symmetric part remains. Under this assumption, covariant derivatives commute, $\nabla_\alpha \nabla_\beta = \nabla_\beta \nabla_\alpha$. Hence

$$\nabla_\alpha N^{\alpha\beta} = \varepsilon^{\alpha\gamma} \nabla_\alpha \nabla_\gamma (\varepsilon^{\beta\delta} \nabla_\delta \chi) = 0. \quad (\text{S13})$$

Consequently, Eq. (S9) becomes

$$\frac{Eh^3}{12(1-\nu^2)} \Delta^2 w - b_{\alpha\beta} \varepsilon^{\alpha\gamma} \varepsilon^{\beta\delta} \nabla_\gamma \nabla_\delta \chi - \varepsilon^{\alpha\gamma} \varepsilon^{\beta\delta} \nabla_\alpha \nabla_\beta w \nabla_\gamma \nabla_\delta \chi - \Delta p_{\text{ol}} = 0. \quad (\text{S14})$$

The Airy stress function fulfills an additional compatibility equation. The stretching strain can be written in terms of stretching stress

$$E_{\alpha\beta} = \frac{1}{Eh} [(1+\nu)N_{\alpha\beta} - \nu g_{\alpha\beta} N^\gamma_\gamma]. \quad (\text{S15})$$

Acting $\varepsilon^{\alpha\gamma} \varepsilon^{\beta\delta} \nabla_\gamma \nabla_\delta$ on Eqs. (S15) and (S4), we obtain the compatibility equation

$$\frac{1}{Eh} \Delta^2 \chi + b_{\alpha\beta} \varepsilon^{\alpha\gamma} \varepsilon^{\beta\delta} \nabla_\gamma \nabla_\delta w + \frac{1}{2} \varepsilon^{\alpha\gamma} \varepsilon^{\beta\delta} \nabla_\alpha \nabla_\beta w \nabla_\gamma \nabla_\delta w = 0. \quad (\text{S16})$$

For spherical shell, $b_{\alpha\beta} = g_{\alpha\beta}/R_0$. The Euler-Lagrange Eqs. (S14) and (S16) become [1]

$$\frac{Eh^3}{12(1-\nu^2)} \Delta^2 w - \frac{1}{R_0} \Delta \chi - \varepsilon^{\alpha\gamma} \varepsilon^{\beta\delta} \nabla_\alpha \nabla_\beta w \nabla_\gamma \nabla_\delta \chi - \Delta p_{\text{ol}} = 0, \quad (\text{S17})$$

$$\frac{1}{Eh} \Delta^2 \chi + \frac{1}{R_0} \Delta w + \frac{1}{2} \varepsilon^{\alpha\gamma} \varepsilon^{\beta\delta} \nabla_\alpha \nabla_\beta w \nabla_\gamma \nabla_\delta w = 0, \quad (\text{S18})$$

which completes the derivation of the Euler-Lagrange equations.

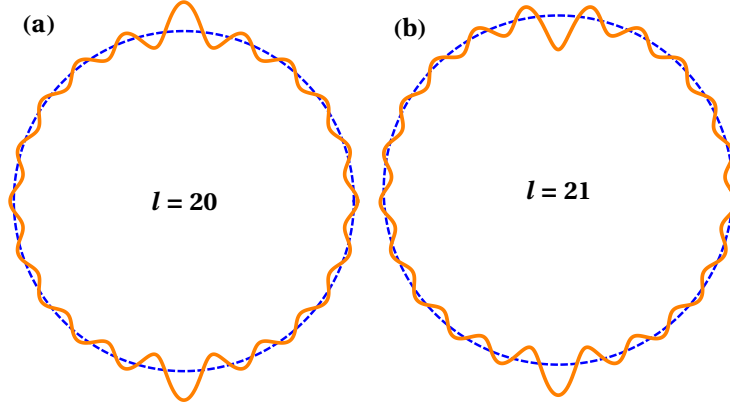


FIG. 1. Schematics of typical wrinkling modes with $\nu = 0.5$. (a) Symmetric mode with $l = 20$ and $R_0/h = 140$. (b) Anti-symmetric mode with $l = 21$ and $R_0/h = 154$.

II. LINEAR STABILITY ANALYSIS OF EULER-LAGRANGE EQUATIONS

In this section, we perform linear stability analysis on Eqs. (S17) and (S18) to find the critical wrinkling pressure. For uniform solution, Eq. (S17) reduces to

$$-\Delta \chi_0 = \Delta p_{\text{ol}} R_0. \quad (\text{S19})$$

Recall that $N^{\alpha\beta} \equiv \varepsilon^{\alpha\gamma} \varepsilon^{\beta\delta} \nabla_\gamma \nabla_\delta \chi$. Then

$$N_{0\alpha}^\alpha = \varepsilon^{\alpha\gamma} \varepsilon_{\alpha\delta} \nabla_\gamma \nabla^\delta \chi_0 = \Delta \chi_0. \quad (\text{S20})$$

There should be $N_{0\phi}^\phi = N_{0\theta}^\theta$ for spherical shell in uniform solution. So

$$N_{0\phi}^\phi = N_{0\theta}^\theta = -\frac{1}{2} \Delta p_{\text{ol}} R_0. \quad (\text{S21})$$

According to stretching strain-stress relation Eq. (S15) and the DMV strain-displacement relation Eq. (S4),

$$E_{\theta\theta} = \frac{1}{Eh} [(1 + \nu)N_{\theta\theta} - \nu g_{\theta\theta} N_\gamma^\gamma] = -\frac{1}{R_0} g_{\theta\theta} w_0. \quad (\text{S22})$$

Then

$$w_0 = -\frac{R_0}{Eh} [(1 + \nu)N_\theta^\theta - \nu N_\gamma^\gamma] = \frac{(1 - \nu)\Delta p_{\text{ol}} R_0^2}{2Eh}. \quad (\text{S23})$$

To find the critical pressure leading to wrinkling, we perform linear stability analysis on Eqs. (S17) and (S18). Expanding $w = w_0 + w_1$ and $\chi = \chi_0 + \chi_1$ and keeping terms up to

linear order, we obtain

$$\frac{Eh^3}{12(1-\nu^2)}\Delta^2 w_1 - \frac{1}{R_0}\Delta\chi_1 + \frac{\Delta p_{\text{ol}}R_0}{2}\Delta w_1 = 0, \quad (\text{S24})$$

$$\frac{1}{Eh}\Delta^2\chi_1 + \frac{1}{R_0}\Delta w_1 = 0. \quad (\text{S25})$$

Note spherical harmonics $Y_l^m(\phi, \theta)$ are eigenmodes of Laplace operator Δ . Substitution of $w_1 = AY_l^m$ and $\chi_1 = BY_l^m$ into the above equations gives us

$$\left[\frac{Eh^3}{12(1-\nu^2)}x - \frac{\Delta p_{\text{ol}}R_0}{2} \right] A + \frac{1}{R_0}B = 0, \quad (\text{S26})$$

$$-\frac{1}{R_0}A + \frac{1}{Eh}xB = 0, \quad (\text{S27})$$

where $x \equiv l(l+1)/R_0^2$. To have non-zero solution of A and B , there must be

$$\frac{Eh^3}{12(1-\nu^2)}x^2 - \frac{\Delta p_{\text{ol}}R_0}{2}x + \frac{Eh}{R_0^2} = 0. \quad (\text{S28})$$

The minimal Δp_{ol} to have a real and positive x corresponds to the critical wrinkling pressure [1]

$$p_w^* = \frac{2E}{\sqrt{3(1-\nu^2)}} \left(\frac{h}{R_0} \right)^2. \quad (\text{S29})$$

In Fig. 1, we have shown two typical wrinkling modes at the critical wrinkling pressure.

III. DERIVATION OF THE PRESSURE IN THE CAVITY p_c

In this section, the pressure in cavity is derived. The equilibrium condition between liquid and cavity is

$$\mu_c(T, p_c) = \mu_l(T, p_l), \quad p_c = p_l + \frac{2\gamma}{R_c}, \quad (\text{S30})$$

where μ_c , μ_l , p_c and p_l are, respectively, chemical potentials and pressures of cavity and liquid. By assuming the gas in cavity is ideal and liquid is incompressible, we have

$$\mu_c(T, p_c) = \mu_c^0(T) + k_B T \ln p_c, \quad (\text{S31})$$

$$\mu_l(T, p_l) = \mu_l^0(T) + p_l v_l, \quad (\text{S32})$$

where v_l is the specific volume of liquid molecule. Then

$$\mu_c^0(T) + k_B T \ln p_c = \mu_l^0(T) + \left(p_c - \frac{2\gamma}{R_c} \right) v_l. \quad (\text{S33})$$

Let $p_{\text{eq}}(T)$ be the solution of Eq. (S33) when $R_c \rightarrow \infty$. Eq. (S33) becomes

$$k_B T \ln \left(\frac{p_c}{p_{\text{eq}}} \right) = (p_c - p_{\text{eq}})v_l - \frac{2\gamma}{R_c}v_l. \quad (\text{S34})$$

Thus

$$p_c = -\frac{k_B T}{v_l} W_0 \left(-\frac{p_{\text{eq}} v_l}{k_B T} e^{-\frac{p_{\text{eq}} v_l}{k_B T} - \frac{2\gamma v_l}{R_c k_B T}} \right), \quad (\text{S35})$$

where W_0 is Lambert W function. Note that the specific volume of water molecule is $3 \times 10^{-29} \text{m}^3$. So $p_{\text{eq}} v_l / (k_B T) \sim 10^{-3}$ and Eq. (S35) can be approximated by

$$p_c \approx p_{\text{eq}} \exp \left(-\frac{2\gamma v_l}{R_c k_B T} \right). \quad (\text{S36})$$

We now estimate the order of the exponential argument. Recall that the surface tension of distilled water at room temperature is $\gamma = 7.2 \times 10^{-2} \text{N/m}$. The specific volume of water molecule is $v_l = 3 \times 10^{-29} \text{m}^3$. The effective osmotic modulus is of the order $K_e \sim 1 \text{ GPa}$. The typical initial radius of droplet in experiment $R_0 \sim 10^{-6} \text{m}$. If we assume the thickness of shell is $h = 0.01 R_0$, then $2\gamma v_l / (R_c k_B T) \sim 10^{-2.75} \ll 1$. If we allow K_e and h to vary and require $2\gamma v_l / (R_c k_B T) < 0.1$, then $v_c > 10^{-6}$ or equivalently $l_e / (2h) > 10^{-8}$, which should be easily fulfilled. Hence

$$p_c \approx p_{\text{eq}} \left(1 - \frac{2\gamma v_l}{R_c k_B T} \right). \quad (\text{S37})$$

Assume $p_o = p_{\text{eq}} = 1 \text{ atm}$. Then $\Delta p_{\text{oc}} = 2\gamma p_{\text{eq}} v_l / (R_c k_B T)$.

IV. DERIVATION OF ELASTIC FREE ENERGY UNDER UNIFORM CONTRACTION

In this section, we derive the elastic free energy under uniform contraction before wrinkling and cavitation. Under uniform contraction with tangential displacement zero and normal displacement w_0 , the bending strain is zero and stretching strain reduces to $E_{\alpha\beta} = -g_{\alpha\beta} w_0 / R_0$, according to the DMV strain-displacement relations in Eqs. (S4) and (S5). Then Helmholtz elastic free energy is

$$F_{\text{elastic}} = \int_S dS \frac{Eh}{2(1-\nu^2)} \left[(1-\nu) E^{\alpha\beta} E_{\alpha\beta} + \nu (E_\gamma^\gamma)^2 \right] = 12\pi h K_e w_0^2, \quad (\text{S38})$$

where an effective osmotic modulus $K_e = E / [3(1-\nu)]$ is introduced.

V. DERIVATION OF HELMHOLTZ FREE ENERGY WITH WRINKLING

In this section, we give the detailed derivation of Helmholtz free energy after wrinkling. The wrinkling is assumed to be in the eigenmode $w = w_0 + AY_l^m$ and the variation of tangential displacement $\nabla_\alpha u_\beta$ is small. Substitution of this solution into the total Helmholtz free energy of the system leads to

$$F_{\text{tot}} = 12\pi K_e h w_0^2 + A^2 \left[\frac{h^3 K_e l^2 (l+1)^2}{8(1+\nu)R_0^2} - \frac{3hK_e w_0 l(l+1)}{2R_0} \right] + 4\pi R_0^2 \gamma v_c^{2/3}. \quad (\text{S39})$$

In the linear instability analysis, we know

$$\frac{l(l+1)}{R_0^2} = \frac{\Delta p_{\text{ol}} R_0}{4D} \left(1 \pm \sqrt{1 - \frac{16DEh}{(\Delta p_{\text{ol}})^2 R_0^4}} \right), \quad (\text{S40})$$

where $D \equiv Eh^3/[12(1-\nu^2)]$. The pressure of near wrinkling onset is $\Delta p_{\text{ol}} \simeq p_c$. Then expansion around $\Delta p_{\text{ol}} = p_c^*$ and keep up to linear term of $\Delta p_{\text{ol}} - p_c^*$ gives us

$$\frac{l(l+1)}{R_0^2} \simeq \frac{\Delta p_{\text{ol}} R_0}{4D}. \quad (\text{S41})$$

The mass conservation relation reads

$$\int_S w \, dS = 4\pi R_0^2 w_0 = \frac{4\pi R_0^3}{3} \left(\frac{\Delta W}{W_0} - v_c \right). \quad (\text{S42})$$

Recall that $w_0 = (1-\nu)\Delta p_{\text{ol}} R_0^2/(2Eh)$. Then

$$\frac{l(l+1)}{R_0^2} = \frac{2(1+\nu)}{h^2} \left(\frac{\Delta W}{W_0} - v_c \right). \quad (\text{S43})$$

Finally we arrive at

$$F_{\text{tot}} = \frac{4\pi R_0^2 h K_e'}{3} \left(v_c - \frac{\Delta W}{W_0} \right)^2 + 4\pi R_0^2 \gamma v_c^{2/3}, \quad (\text{S44})$$

where $K_e' = K_e[1 - 3(1+\nu)A'^2/(8\pi)]$ and $A' = A/h$.

VI. OCCURRENCE CONDITIONS OF PHASES

Occurrence conditions of four possible phases on the drying pathways are listed as follows.

- No cavitation or wrinkling:

$$\frac{\Delta W}{W_0} < \min \left\{ 2^{1/4} \left(1 + \frac{p_{\text{eq}} v_l}{2k_B T} \right) \left(\frac{l_e}{h} \right)^{3/4}, \sqrt{\frac{3(1-\nu)}{1+\nu}} \frac{h}{R_0} \right\}. \quad (\text{S45})$$

- Cavitation only:

$$\frac{\Delta W}{W_0} > 2^{1/4} \left(1 + \frac{p_{\text{eq}} v_l}{2k_B T} \right) \left(\frac{l_e}{h} \right)^{3/4}$$

and $2^{1/4} \left(1 + \frac{p_{\text{eq}} v_l}{2k_B T} \right) \left(\frac{l_e}{h} \right)^{3/4} < \sqrt{\frac{3(1-\nu)}{1+\nu}} \frac{h}{R_0}.$ (S46)

- Wrinkling only:

$$\sqrt{\frac{3(1-\nu)}{1+\nu}} \frac{h}{R_0} < \frac{\Delta W}{W_0} < 2^{1/4} \left(1 + \frac{p_{\text{eq}} v_l}{2k_B T} \right) \left(\frac{l'_e}{h} \right)^{3/4}$$

and $2^{1/4} \left(1 + \frac{p_{\text{eq}} v_l}{2k_B T} \right) \left(\frac{l_e}{h} \right)^{3/4} > \sqrt{\frac{3(1-\nu)}{1+\nu}} \frac{h}{R_0}.$ (S47)

- Wrinkling and cavitation:

$$\frac{\Delta W}{W_0} > 2^{1/4} \left(1 + \frac{p_{\text{eq}} v_l}{2k_B T} \right) \left(\frac{l'_e}{h} \right)^{3/4}$$

and $2^{1/4} \left(1 + \frac{p_{\text{eq}} v_l}{2k_B T} \right) \left(\frac{l_e}{h} \right)^{3/4} > \sqrt{\frac{3(1-\nu)}{1+\nu}} \frac{h}{R_0}.$ (S48)

[1] F. Niordson, *Shell Theory* (Nord-Holland, Amsterdam, 1985).